HHS Public Access

Author manuscript

Transl Stroke Res. Author manuscript; available in PMC 2023 October 01.

Published in final edited form as:

Transl Stroke Res. 2022 October ; 13(5): 801–815. doi:10.1007/s12975-022-00992-y.

Compartmentalized actions of the plasminogen activator inhibitors, PAI-1 and Nsp in ischemic stroke

Daniel Torrente[1,‡], **Enming Joseph Su**[2,‡], **Linda Fredriksson**[3], **Mark Warnock**[2], **David Bushart**[2,4], **Kris Mann**[2], **Cory D. Emal**[5], **Daniel A. Lawrence**[1,2,*]

[1]Department of Molecular and Integrative Physiology, University of Michigan Medical School, Ann Arbor, Michigan, USA.

[2]Department of Internal Medicine, Division of Cardiovascular Medicine, University of Michigan Medical School, Ann Arbor, Michigan, USA.

[3]Department of Medical Biochemistry and Biophysics, Division of Vascular Biology, Karolinska Institute, Scheeles v. 2, 17177, Stockholm, Sweden.

[4]Current affiliation: Ohio State University College of Medicine, Columbus, Ohio, USA.

[5]Department of Chemistry, Eastern Michigan University, Ypsilanti, Michigan 48197

Abstract

Tissue plasminogen activator (tPA) is a multifunctional protease. In blood tPA is best understood for its role in fibrinolysis, whereas in the brain tPA is reported to regulate blood brain barrier (BBB) function and to promote neurodegeneration. Thrombolytic tPA is used for the treatment of ischemic stroke. However, its use is associated with an increased risk of hemorrhagic transformation. In blood the primary regulator of tPA activity is plasminogen activator inhibitor 1 (PAI-1), whereas in the brain, its primary inhibitor is thought to be neuroserpin (Nsp). In this study, we compare the effects of PAI-1 and Nsp deficiency in a mouse model of ischemic stroke and show that tPA has both beneficial and harmful effects that are differentially regulated by PAI-1 and Nsp. Following ischemic stroke Nsp deficiency in mice leads to larger strokes, increased BBB permeability, and increased spontaneous intracerebral hemorrhage. In contrast, PAI-1 deficiency

[*]Address correspondence to: Daniel A. Lawrence, 7301 MSRB III, 1150 W. Medical Center Dr., Ann Arbor MI 48109-0644., Tel.: Phone: 734-763-7838; Fax: 734-936-2641; dlawrenc@umich.edu.

[‡]These authors contributed equally to this study.

Authors' contributions

DT, EJS, LF, MW, DB, KM conducted experiments and analyzed data, CDE synthesized MDI-2268, DT, EJS, DAL conceived the study and analyzed data and participated in writing the manuscript.

Competing interests

Daniel A. Lawrence is a member of the board and holds equity in MDI Therapeutics which is developing therapeutic inhibitors of PAI-1, and which holds an option to license MDI-2268. Enming Joseph Su and Cory D. Emal hold equity in MDI Therapeutics. All other authors report that they have no conflicts of interest.

Declarations

Ethics approval and consent to participate

No human subjects were involved. All animal experiments were approved by the Institutional Animal Care and Use Committee of Unit for Laboratory Animal Medicine at the University of Michigan.

Consent for publication

All authors have reviewed than manuscript and approve its content and consent to publication.

Availability of data and material

All data generated or analyzed during this study are included in this published article [and its supplementary information files].

results in smaller infarcts and increased cerebral blood flow recovery. Mechanistically, our data suggests that these differences are largely due to the compartmentalized action of PAI-1 and Nsp; with Nsp deficiency enhancing tPA activity in the CNS which increases BBB permeability and worsens stroke outcomes, while PAI-1 deficiency enhances fibrinolysis and improves recovery. Finally, we show that treatment with a combination therapy that enhances endogenous fibrinolysis by inhibiting PAI-1 with MDI-2268 and reduces BBB permeability by inhibiting tPA-mediated PDGFRα signaling with imatinib, significantly reduces infarct size compared to vehicle-treated mice and to mice with either treatment alone.

Keywords

tPA; ischemic stroke; Neuroserpin; imatinib; MDI-2268

Introduction

Stroke is one of the leading causes of morbidity and mortality worldwide [1]. Approximately 87% of acute strokes are ischemic with the rest being hemorrhagic [2]. Outcomes for hemorrhagic strokes are more severe than for ischemic strokes and hemorrhagic transformation of an ischemic stroke markedly increases stroke mortality [3, 4]. Currently, thrombolytic therapy with intravenous tissue plasminogen activator (tPA) is the only FDA-approved pharmaceutical treatment for ischemic stroke. Intravenous tPA promotes cerebral blood flow recovery by the enzymatic conversion of plasminogen to plasmin leading to fibrin degradation and breakdown of the occluding thrombus [5]. Although the benefits of thrombolytic treatment with tPA for early blood flow restoration in stroke patients is well established, the increased risk of hemorrhagic transformation is a significant limiting factor for its use [5, 6].

The blood-brain barrier (BBB) is required to maintain a tight control in the trafficking of molecules between the blood and the central nervous system (CNS) [7]. However, during ischemic stroke, dysfunction of the BBB occurs which can intensify neuronal damage in the ischemic penumbra and increase the risk of hemorrhagic transformation [8]. Previously, we have shown that perivascular tPA in the brain increases BBB permeability [9], via tPA-mediated activation of latent platelet-derived growth factor CC (PDGF-CC) and subsequent signaling through the PDGF receptor α (PDGFRα) [10–12]. We also showed that blocking this pathway in a mouse model of ischemic stroke significantly reduces hemorrhagic transformation associated with late tPA-mediated thrombolysis administered 5 hours after middle cerebral artery occlusion (MCAO) [10, 12]. Significantly, a recent phase II clinical trial targeting this pathway in ischemic stroke patients receiving thrombolytic tPA demonstrated that the PDGFRα inhibitor imatinib was safe and tolerable and may reduce neurologic disability in patients treated with intravenous thrombolysis [13].

The compartmentalization of tPA in the blood and the CNS is maintained by the BBB, which permits tPA in the blood to promote beneficial fibrinolysis through the activation of plasminogen, without activating PDGF-CC-PDGFRα signaling in the CNS which can lead to BBB disruption and ultimately to hemorrhagic transformation. Thus, in ischemic stroke

tPA has the potential for both beneficial and harmful activities that are governed at least in part by tPA's location and potential substrates. It is well established that in the blood, tPA activity is controlled by plasminogen activator inhibitor 1 (PAI-1) [14] and in the CNS it is thought that the related inhibitor, neuroserpin (Nsp) is a primary regulator of tPA activity [11, 15, 16]. Therefore, in the present study, we have investigated the differential function of the tPA inhibitors, PAI-1 and Nsp in fibrinolysis, BBB regulation, and hemorrhagic transformation in a photothrombotic MCAO mouse model of ischemic stroke with the goal to identify non-overlapping pathways mediated by tPA that have therapeutic potential for improving the treatment of ischemic stroke. We found that deficiency of PAI-1 increases beneficial endogenous fibrinolysis whereas Nsp deficiency leads to BBB dysfunction and intracerebral hemorrhage (ICH) primarily mediated by tPA's action. Furthermore, combined pharmacological inhibition of PAI-1 and the tPA-mediated PDGFRα-signaling pathway showed additive protection in stroke compared to the individual inhibition of either pathway.

Methods

Ischemic stroke model

Male WT (C57BL/6J; Jackson Laboratory), Nsp$^{-/-}$ [17], PAI-1$^{-/-}$ [18], and Nsp/tPA$^{-/-}$ (8–15 weeks old) mice were subjected to a photothrombotic MCAO stroke model previously described [10, 12]. The Nsp/tPA$^{-/-}$ mice were generated by crossing the Nsp$^{-/-}$ mice with tPA$^{-/-}$ mice [19], and all knockout strains were backcrossed more than 10 generations onto the C57BL/6J background. Briefly, mice were anesthetized with chloral hydrate (450mg/kg), and using a dissecting microscope the left middle cerebral artery (MCA) was exposed. Then, Rose Bengal (Fisher) was injected intravenously (50 mg/kg) while a 3.5-mW green light laser (540 nm, Melles Griot) was directed at the exposed MCA. A laser Doppler flow probe (Type N, Transonic Systems) connected to a flowmeter (Transonic model BLF21) was used to record the relative tissue perfusion units 1.5 mm dorsal median from the bifurcation of the MCA. Stable occlusion was achieved when the tissue perfusion units dropped to less than 20% of pre-occlusion levels and did not rebound within 10 min after laser withdrawal [10, 12]. Tissue perfusion continuous data acquisition was done using Windaq data Acquisition software (DATAQ instruments). All animal experiments were approved by the Institutional Animal Care and Use Committee of Unit for Laboratory Animal Medicine at the University of Michigan. In accord with the STAIR recommendations for preclinical studies in all experiments sample sizes were calculated from preliminary studies or historical data, mice were randomized into treatment groups (or by genotype), and were only excluded for a predefined cause. Data analysis was performed by an investigator blinded to the experimental conditions until the results were decoded by a senior investigator after analysis.

Drug treatments

Treatment agents were delivered as follows: Aprotinin (Abcam) was injected I.P. 1h after MCAO at 10mg/kg twice daily for 3 days. MDI-2268 was synthesized as described [20] and injected I.P. at 3mg/kg twice daily for 3 days starting 30 min after MCAO. Imatinib (Gleevec) was delivered via oral gavage 30 min after MCAO at 300 mg/kg twice daily for 1 or 3 days. The same treatment regimen was administered in all combination therapy experiments using MDI-2268 and imatinib. MDI-2268 and imatinib total daily dosages were

selected based on previous studies [11, 20]. Human tPA (Alteplase) was delivered slowly via tail vein 5 h after MCAO at 10mg/kg.

Cerebral blood flow measurements

All Cerebral Blood flow (CBF) measurements were started 10min before Rose Bengal injection on the mouse exposed skull using a full-field laser speckle imaging device (moorFLPI-2). Mice were anesthetized with chloral hydrate (450mg/kg) and secured on a stereotactic frame pre-MCAO and 24 h after MCAO. CBF images were acquired for a total of 40-sec in 10-sec intervals with an exposure time of 20-ms. Pre-MCAO CBF measurements were considered baseline levels and the average CBF over 40-sec was considered 100% and used to normalize CBF data 24h after MCAO in WT, $Nsp^{-/-}$ and $PAI\text{-}1^{-/-}$ mice. For CBF measurements 24h after MCAO mice were re-anesthetized with 2% isoflurane and CBF data was acquired in the same region. CBF image analysis was performed in MoorFLPI Review V 4.0 software (Moor Instruments).

Infarct size

Infarct size analysis was performed as described previously [10, 12]. Briefly, brains were removed 72 h after MCAO and 2-mm thick coronal sections of the whole brain were stained with 4% 2,3,5-triphenyltetrazolium chloride (TTC) in PBS for 20min at 37°C. Images of TTC stained sections were captured with an Olympus digital C-3030 color camera attached to an SZ-60 Olympus microscope. The sections were analyzed with NIH Image J software using the following formula:

$$V_{\%infarct} = \sum(\text{Areas of lesion}) / \sum(\text{Areas of ipsilateral hemisphere}) * 100,$$

where $V_{\%infarct}$ is infarct size calculated as percent of the ipsilateral hemisphere.

Hemorrhage volume

For assessment of hemorrhagic volume in the brain, digital images (both sides) were captured (using the same coronal sections in TTC staining) before brain sections were fully developed in TTC solutions. Images were analyzed using the Image J software (NIH) by an investigator blind to the treatments as described in [12]. The following formula was used to calculate hemorrhagic volume:

$$V_{ICH} = (\sum \left(\text{Areas of ICH}(mm^2)/2\right) \times 2mm$$

Where V_{ICH} is ICH volume calculated in cubic millimeters.

FITC-Fibrinogen quantification

FITC-conjugated mouse fibrinogen (0.3mg/kg) was injected intravenously 10mins before MCAO, mice were PBS and PFA-perfused 3 h after MCAO. Brains were removed and side view images of the whole intact mouse brain 3h after MCAO were captured using an Olympus SZX16 fluorescence stereo microscope. These images were used for the quantification of FITC-fibrinogen deposition in cortical regions of the whole

stroked hemisphere of WT, Nsp$^{-/-}$ and PAI-1$^{-/-}$ mice 3 h after MCAO. FITC-fibrinogen fluorescence intensity of the stroked hemisphere was quantified using NIH Image J software. Brightness and contrast settings were changed and applied equally to all images to generate the final image.

Evans blue assay

For analysis of BBB permeability after MCAO, we used an assay previously described [10, 12]. Briefly, mice were injected with 100 μL of 4% Evans blue (Sigma-Aldrich) intravenously 23 h after MCAO and 1h later, animals were PBS-perfused for 8 min. The brains were harvest and split into ipsilateral and contralateral hemispheres relative to MCAO. Each hemisphere was then homogenized in N, N-dimethylformamide (Sigma-Aldrich) and centrifuged for 45 min at 25,000 g. The supernatants were collected, absorbances were measured at 500, 620 and 740 nm using a spectrophotometer (Spectramax M5 or Spectramax ID5). EB extravasation in each hemisphere was quantified from the formula: (A620 nm − ((A500 nm + A740 nm)/2))/mg wet weight [10, 12].

Immunohistochemistry

For immunofluorescence, WT naïve brains were PBS and PFA-perfused, brains were harvest and post-fixed in PFA and cryopreserved in 30% sucrose. Fourteen μm-thick frozen sections were permeabilized in 0.5% TritonX-100 and nonspecific binding blocked using TNB blocking buffer (NEL700A001KT, Perkin Elmer, Waltham, MA, USA) or 1% Bovine Serum Albumin (BSA) in 0.5% TritonX-100/PBS. Sections were incubated with primary antibodies in blocking solution overnight at 4°C followed by incubation with Alexa-Fluor conjugated secondary antibodies for 45 min, room temperature. The primary antibodies and their respective dilution used were: tPA (12 μg/mL, rabbit HTMTPA and goat SHTMTPA, Molecular Innovations, Novi, MI, USA), Nsp (15 μg/mL, rabbit HTmNs; Lawrence Lab), Podocalyxin (1:200, AF1556; R&D Systems, Minneapolis, MN, USA). For tPA and Nsp staining, heat-mediated antigen retrieval was performed using DAKO retrieval solution (S1700; DAKO, Glostrup, Denmark). The sections were mounted using ProLong Gold Antifade reagent (P36930; Life Technologies). Brain sections from tPA$^{-/-}$ and Nsp$^{-/-}$ mice were used for antibody control and demonstrated that both antibodies were specific for their respective antigen. All images were acquired in RT with a Zeiss LSM510 alternatively LSM700 confocal microscope and the ZEN 2009 software (Carl Zeiss, Oberkochen, Germany). The images are representative of the respective staining and were processed and analyzed using Volocity 3D image analysis software (PerkinElmer) and Photoshop CS5 (Adobe, San Jose, CA, USA). Brightness and contrast settings were changed and applied equally to all images to generate the final image.

RT-PCR assay

RNA was isolated from PBS-perfused WT naïve mouse brains using QIAzol lysis buffer with the RNeasy kit (Qiagen) following manufactured instructions. Quantitative RT-PCR analysis was performed using TaqMan® One-Step RT-PCR Kit and TaqMan® Gene Expression Assays according to Applied Biosystems instructions. FAM-labeled primers for tPA (*PLAT*; Mm00476931_m1), Nsp (*SERPINI1*; Mm00436740_m1) and PAI-1 (*SERPINE1*; Mm00435858_m1) were obtained from ThermoFisher. Fold Change

gene expression was expressed relative to the housekeeping gene Beta-Actin (*ACTB;* Mm00607939_s1) and corrected for primer efficiencies (tPA: 2.08; Nsp: 1.98; PAI-1: 1.91).

tPA, Nsp and PAI-1 protein measurements

Levels of tPA, Nsp and PAI-1 in plasma and brain extracts of naïve WT mice were measured using either ELISA or Luminex assays. Plasma samples were collected from the *inferior vena cava* using 3.2% sodium citrate buffer as an anticoagulant. After, plasma collection, animals were PBS-perfused, and brains were collected, homogenized and extracted in a HEPES buffer solution (0.4M HEPES, 0.1M NaCl; 1% Triton X-100, pH 7.4).

tPA measurements: For tPA levels in the brain and plasma, we used a Luminex assay described in detail previously [21]. Briefly, rabbit anti-mouse tPA (Molecular Innovations, ASMTPA-GF-HT) was coupled to carboxylated beads (Luminex). The beads were then incubated for 2h in filter plate (Millipore MABVN0B50) at room temperature in the dark with either brain or plasma samples, washed and a biotin-labeled rabbit anti-mouse tPA antibody (Molecular Innovations, ASHTPA-HT) was added for 1h at room temperature. The beads were then washed and streptavidin linked R-Phycoerythrin (ThermoFisher Scientific, S866) was added for 30min, the beads were washed again, resuspended in sheath fluid (Luminex) and analyzed. All antibody incubations were followed by three washes of PBS-0.05% Tween 20. The Luminex 100 device was used to detect the fluorescence signal.

Nsp measurements: Nsp levels in brain and plasma were measured by ELISA. A rabbit anti-mouse NSP capture antibody (2 μg/ml; Lawrence Lab) was incubated in high binding microplates in carbonate buffer (0.15M Na_2CO_3, 0.35M $NaHCO_3$, pH 9.6) overnight at 4°C. Following all incubation steps the plates were washed three times with 0.9% Saline-0.05% Tween 20. Mouse brain and plasma samples were loaded and incubated for 2h at RT. A sheep anti-mouse NSP-biotin-labeled (2 μg/ml; Molecular Innovations, SASMNSP-GF-BIO) and Streptavidin-HRP (1:20000; Invitrogen) were used as a primary and secondary antibody, respectively. The ELISA was then developed with the TMB substrate (3,3',5,5'-tetramethylbenzidine, Molecular Innovations), followed by H_2SO_4 (1 N) and the absorbance was measured at 450 nm on a spectrophotometer (Spectramax M5).

PAI-1 measurements: To measure total mouse PAI-1 in brain and plasma samples, a Luminex assay was performed following a previous published protocol [22, 23]. Briefly, anti-mouse PAI-1 (Molecular Innovation clone H34G6) was coupled to carboxylated beads (Luminex). Brain and plasma samples with anti-mouse PAI-1 coupled beads were loaded to a filter plate (Millipore MABVN0B50) and incubated for 2h in the dark. Biotinylated rabbit anti-mouse PAI-1 (2 μg/mL; Molecular Innovations) and phycoerythrin-conjugated streptavidin (ThermoFisher Scientific, S866) were used as a primary and secondary antibody, respectively. The Luminex 100 device was used to detect the fluorescence signal [22, 23].

D-dimer ELISA assay

For D-dimer, citrated plasma was obtained from both naïve WT and PAI-$1^{-/-}$ mice and from each genotype 6 h after MCAO, and D-dimer levels determined following manufactured instructions using the mouse D-dimer (D2D) ELISA Kit (CSB-E13584m; CUSABIO).

Statistical analysis

Data analysis was performed using GraphPad Prism 8 statistical software (GraphPad Software, La Jolla, CA, USA). All experiments were repeated at least two independent times and n indicates the number of individual mice used in the study. For statistical analysis, in any experiment with only two groups, a two-tailed t-test was used. For experiments with more than two groups, a one-way ANOVA with Tukey post hoc test was used. Data is represented as mean values ± SEM; $p < 0.05$ was considered significant.

Results

Expression of tPA, Nsp and PAI-1 in brain and blood

In vivo it is thought that tPA has two main inhibitors, PAI-1 and Nsp, with Nsp expression being largely restricted to the CNS, where PAI-1 expression is relatively low. It has been proposed that Nsp and not PAI-1 is the main inhibitor of tPA in the CNS [15, 16]. To examine this and to confirm previous reports regarding the spatial division of Nsp and PAI-1 in the brain and blood, we performed qPCR expression analysis of PAI-1, Nsp and tPA genes in the brains of naïve WT mice. These data show that the Nsp mRNA level is approximately 5000-fold higher than PAI-1 mRNA in naïve WT brains, and that tPA mRNA level is nearly 100-fold higher than PAI-1 (Fig 1a). To determine if there was a direct correlation between mRNA and protein levels in the mouse brain, we measured PAI-1, Nsp and tPA protein concentrations in whole brain homogenates of naïve WT mice. We found that the Nsp protein level was approximately 12-fold higher than the PAI-1 protein level in naïve WT brains, and that the tPA protein level was nearly 139-fold higher than PAI-1 (Fig 1b). The relative differences between the mRNA expression of tPA and Nsp and their respective protein levels in the brain are likely due to the Nsp single interaction mousetrap-like mechanism and the relatively rapid turnover of Nsp after interaction with tPA [15, 24, 25]. These data support the suggestion that Nsp and not PAI-1 is the primary inhibitor of tPA in the CNS. In contrast, PAI-1 and tPA levels were similar in plasma, whereas Nsp was not detected (Fig 1c), supporting PAI-1 as the main inhibitor of tPA activity in blood. Additionally, to examine tPA and Nsp colocalization in the mouse brain, we performed immunohistochemical staining in cortical brain regions of naïve WT mice. These data show widespread tPA staining both in perivascular regions outside cerebral vessels and associated directly with blood vessels, stained with the endothelial glycocalyx protein podocalyxin (Fig 1d). Nsp staining was also found proximal to blood vessels and tPA (Fig 1e–f). No PAI-1 staining was observed in the cortex parenchyma of naïve WT mice (Supplementary Figure S1).These results are in good agreement with histological evidence showing similar expression patterns of Nsp and tPA in hippocampal regions in the mouse brain [11]. Overall, these data support the hypothesis that Nsp is the primary inhibitor of tPA in the CNS, and PAI-1 is the primary inhibitor of tPA in blood.

Nsp and PAI-1 deficiency have opposite effects on infarct size after MCAO

It is well established that PAI-1 can regulate fibrinolysis in the blood [26, 27] and that early tPA-mediated fibrinolysis is associated with better outcomes after ischemic stroke in humans [28, 29]. However, we have shown that therapeutically administered thrombolytic tPA, especially if administered 5h after the onset of ischemia can induce BBB opening and increase the risk of hemorrhagic transformation in a murine model of ischemic stroke [10, 12]. Based on these observations, we hypothesize that during cerebral ischemia, tPA plays a dual role with both beneficial and harmful effects that are governed by tPA's location and substrates. To test this hypothesis, we subjected WT, PAI-1 (PAI-$1^{-/-}$) and Nsp ($Nsp^{-/-}$) deficient mice to photothrombotic MCAO, and 72h later infarct size was determined. We predict that in PAI-$1^{-/-}$ mice tPA activity will increase in blood, thereby enhancing endogenous fibrinolysis which should reduce stroke severity. Whereas in $Nsp^{-/-}$ mice tPA activity should increase in the CNS parenchyma which would increase BBB damage and worsen stroke severity. Our results demonstrate that as predicted, the effects on infarct size in Nsp and PAI-1 deficient mice are opposite, with PAI-$1^{-/-}$ mice showing a significant reduction in infarct size and mice lacking Nsp with a significant increase in infarct size compared to WT mice (Fig 2a–b).

Nsp deficiency but not PAI-1 deficiency increases BBB opening after MCAO

Since Nsp is likely to be the primary inhibitor of tPA in the CNS (Fig 1 a–f), and our previous studies have shown that tPA activity in the CNS increases BBB opening [9–11], we next examined the effects of Nsp and PAI-1 deficiency on BBB permeability and spontaneous hemorrhage after ischemic stroke. These data show that $Nsp^{-/-}$ mice but not PAI-$1^{-/-}$ mice have a significant increase in BBB disruption compared to WT mice 24h after MCAO. This data is consistent with our previous studies where intracerebroventricular injection of Nsp reduced Evans blue extravasation after MCAO [9]. There was no significant difference in Evans blue dye extravasation between PAI-$1^{-/-}$ and WT mice (Fig 3a–b).

The association of thrombolytic tPA treatment with an increased risk of ICH in stroke patients [6] together with the observation that blocking tPA-induced PDGFRα signaling decreased fibrinolytic tPA-induced ICH [10, 12, 13], suggests that in the CNS tPA may play a critical role in the development of ICH after stroke. To test this hypothesis, we examined spontaneous hemorrhage volume in WT, PAI-$1^{-/-}$ and $Nsp^{-/-}$ mice 72h after MCAO. These data indicate that there is a significant increase in hemorrhage volume in $Nsp^{-/-}$ mice compared to WT and PAI-$1^{-/-}$ mice (Fig 3c–d). These data suggest that unregulated tPA activity in the CNS parenchyma due to Nsp deficiency not only increases BBB permeability but also increases the risk of spontaneous ICH after MCAO, while PAI-1 deficiency has no significant effect on spontaneous ICH.

tPA mediates the increase in infarct size and BBB opening in Nsp deficient mice

To test if the increase in infarct size, ICH and BBB disruption in $Nsp^{-/-}$ mice was mediated by tPA activity we performed MCAO in WT, $Nsp^{-/-}$, and mice deficient in both Nsp and tPA (Nsp/$tPA^{-/-}$). These data show a significant reduction in infarct size, ICH and BBB leakage in Nsp/$tPA^{-/-}$ mice compared to $Nsp^{-/-}$ mice (Fig 4a–c). This confirms that tPA is required for the early BBB leakage and the increases in ICH and infarct size in Nsp deficient

mice. Furthermore, since Nsp/tPA$^{-/-}$ mice also showed a modest reduction in infarct size compared to WT mice, this suggests that the potential harmful effects of endogenous tPA on the BBB may outweigh its potential benefit for increased fibrinolysis.

Since we have previously shown that in WT mice inhibition of PDGFRα prevents tPA-mediated effects on the BBB [10, 11], we examined if tPA-mediated PDGFRα signaling plays a role in the increase in BBB disruption observed in Nsp$^{-/-}$ mice. For this study Nsp$^{-/-}$ mice were treated with the PDGFRα inhibitor imatinib 30 min after MCAO (imatinib; 300 mg/Kg; twice daily). As expected, imatinib treatment significantly reduced Evans blue extravasation in Nsp$^{-/-}$ mice compared to vehicle-treated mice (Fig 4d). These results confirm that as in WT mice [10], the BBB phenotype observed in Nsp$^{-/-}$ mice is mediated by tPA-PDGFRα signaling.

PAI-1 deficiency improves reperfusion after MCAO by increasing fibrinolysis

Previous studies in both rats and mice have demonstrated that following MCAO there is an expansion of the infarct size that is due to the development of fibrin rich microvascular thromboses that are secondary to the primary MCAO [30–32]. Since PAI-1 is the primary inhibitor of both tPA and the other plasminogen activator in blood, urokinase plasminogen activator (uPA), [14] then PAI-1 deficiency should enhance endogenous fibrinolysis after MCAO, and may reduce infarct expansion by limiting the development of secondary thrombosis. In contrast, Nsp deficiency would not be expected to affect fibrinolysis in the blood since it is primarily expressed in the CNS (Fig 1). To test this, we examined cortical regions of the ischemic penumbra for possible microvascular thrombosis by fluorescence stereo microscopy. For this analysis, we first injected WT mice intravenously with FITC-conjugated fibrinogen (0.3mg/kg) 10min before inducing MCAO and performed a time course examining fibrin deposition. Mice were perfused at either 0 (no MCAO), 1, 3 or 6h after MCAO Supplementary Figure S2a). These data indicated that there was a significant increase in FITC-fibrin deposition in the brain over time from 1 to 3h after MCAO, reaching a plateau between 3 and 6h after MCAO. Closer examination of coronal sections of the stroked hemisphere showed FITC-fibrin positive clots in microvessels predominantly located in the periphery of the infarct, suggesting that secondary thrombosis was occurring in the ischemic penumbra where CBF may be reduced (Supplementary Figure S2b–c). We next examined if the FITC-fibrin deposition in the ischemic hemisphere was different between WT, PAI-1$^{-/-}$ and Nsp$^{-/-}$ mice 3h after MCAO. This time point was selected based on the time-course experiment in WT mice Supplementary Figure S2a). These data showed a significant reduction in FITC-fibrin deposition in PAI-1$^{-/-}$ mice compared to that in WT and Nsp$^{-/-}$ mice. As expected Nsp$^{-/-}$ mice showed no significant difference in FITC-fibrin deposition compared to WT mice (Fig 5a–b). We then examined if the early decrease in FITC-fibrin deposition in PAI-1$^{-/-}$ mice was associated with improved cerebral blood flow (CBF). To test this, we measured CBF 24h after MCAO in WT, PAI-1$^{-/-}$ and Nsp$^{-/-}$ mice using full-field laser speckle imaging. We found that relative to WT mice, PAI-1$^{-/-}$ but not Nsp$^{-/-}$ mice had significantly improved CBF 24h after MCAO (Fig 5c–d). In agreement with the FITC-fibrin deposition data, there was no significant difference in CBF between WT and Nsp$^{-/-}$ mice, suggesting that Nsp is not directly involved in fibrinolysis and reperfusion during MCAO.

To determine if the improved perfusion observed in the peri-infarct zone in PAI-$1^{-/-}$ mice was due to enhanced endogenous fibrinolysis, the relative extent of endogenous fibrinolysis in WT and PAI-$1^{-/-}$ mice was examined by ELISA for plasma D-dimer levels 6h after MCAO. D-dimer is a breakdown product of fibrin that is generated by plasmin cleavage of fibrin clots. Our data indicate that PAI$1^{-/-}$ mice show a significant increase in plasma D-dimer levels 6h after MCAO compared to WT mice 6h after MCAO and naïve WT and PAI-$1^{-/-}$ mice (Fig 5e). To confirm if the apparent enhanced endogenous fibrinolysis was the primary mechanism responsible for the reduced infarct size observed in PAI-$1^{-/-}$ mice, we treated PAI-$1^{-/-}$ mice with the potent fibrinolytic inhibitor aprotinin beginning 1h after MCAO (aprotinin: 10mg/kg, twice daily for 3 days), and infarct volumes were determined 72h after MCAO. We found that aprotinin-treated PAI-$1^{-/-}$ mice showed a significant increase in infarct size compared with vehicle-treated PAI-$1^{-/-}$ mice 72h after MCAO (Fig 5f). These data confirm that enhanced endogenous fibrinolysis in PAI-$1^{-/-}$ mice is likely responsible for their reduced infarct size relative to WT mice after MCAO.

Combined pharmacological inhibition of PAI-1 and tPA-Nsp pathway shows additive protection of the infarct zone after MCAO in WT mice

We have shown that tPA activity in the brain and fibrinolysis in the blood regulate two independent pathways relevant to ischemic stroke outcomes. This suggests that a combination therapy that targets both tPA-mediated BBB damage in the brain, by blocking PDGFRα signaling, and promoting endogenous fibrinolytic activity in blood, by inhibiting PAI-1, might lead to an additive or synergistic beneficial effect after ischemic stroke. To determine if combined inhibition of PAI-1 and PDGFRα signaling have beneficial effects after MCAO, a novel small molecule with potent anti-PAI-1 activity (MDI-2268) [20] and the PDGFRα inhibitor imatinib were administered to WT mice 30 min after MCAO (MDI-2268: 3mg/kg I.P., twice daily for 3 days; imatinib: 300mg/kg by oral gavage, twice daily for 3 days). Infarct volume and spontaneous hemorrhage volume were then evaluated 72h after MCAO. These data show that both MDI-2268-treated or imatinib-treated WT mice have significantly reduced infarct sizes compared to vehicle-treated WT mice. Additionally, combined treatment of MDI-2268 plus imatinib shows a significant reduction in infarct size compared to MDI-2268 or imatinib treatment alone (Fig 6a). None of the treatments significantly increased ICH suggesting that they are not only effective but are also safe (Fig 6b). Together, these data suggest that a combined therapeutic approach targeting both PAI-1 and tPA-mediated PDGFRα signaling may be a safe and effective approach to treat ischemic stroke.

Finally, to explore if the dual treatment of MDI-2268 plus imatinib is safe in combination with the currently approved therapy for ischemic stroke, intravenous tPA, we treated WT mice with MDI-2268 and imatinib as described above followed by thrombolysis with intravenous tPA (10 mg/kg) 5h after MCAO. We selected tPA treatment 5h after MCAO to test if the combination therapy of MDI-2268 and imatinib affected the risk of ICH associated with thrombolysis since this risk is known to increase with elapsed time after stroke onset in both humans [33] and rodents [34]. Infarct volume and spontaneous hemorrhage volume were evaluated 72h after MCAO. We found that combined treatment of MDI-2268 plus imatinib followed by delayed tPA treatment reduces infarct size compared to WT mice

treated with late tPA alone. No significant difference in infarct size was observed between WT mice treated with tPA alone and WT vehicle-treated mice after MCAO (Fig 6c). This data is consistent with previous studies showing no effect on infarct size with delayed tPA treatment in WT mice after MCAO [10, 35]. However, as shown previously [12] late fibrinolysis with tPA in WT mice 5h after MCAO results in a significant increase in ICH compared to vehicle-treated WT mice. Interestingly, the combined treatment of MDI-2268 plus imatinib followed by late tPA treatment significantly reduces ICH compared to WT mice treated with late tPA only (Fig 6d). This data indicates that the combination treatment of MDI-2268 with imatinib is not only safe in the context of thrombolysis with tPA, but also shows a significant reduction in stroke severity compared to late tPA treatment alone.

Discussion

The current standard of care for moderate to severe ischemic stroke is thrombolytic therapy with tPA [36], and treatment with tPA can significantly improve neurological outcomes [37]. However, thrombolytic therapy with tPA is also associated with an increased risk of ICH, and due in part to the risk of hemorrhagic transformation, it is estimated that less than 10% of ischemic stroke patients receive intravenous tPA, while 1–2% receive intra-arterial therapy [36, 38]. Therefore, understanding the mechanisms driving the increased risk of hemorrhage associated with tPA could significantly improve stroke treatment. In this study, we examined the differential functions of two endogenous tPA inhibitors, PAI-1 and Nsp in a photothrombotic model of stroke. We showed that during ischemic stroke endogenous tPA has both beneficial and harmful effects that are differentially regulated by the actions of PAI-1 and Nsp. We found that Nsp deficiency leads to larger infarct sizes by increasing BBB leakage and spontaneous ICH through the action of tPA-induced PDGFRα signaling. In contrast, PAI-1 deficiency showed protection by enhancing fibrinolysis and improving CBF recovery. We also found that PAI-1 does not affect BBB integrity or hemorrhagic events following ischemic stroke, while Nsp does not regulate vascular fibrinolysis. Finally, we demonstrated that a combination therapy targeting both PAI-1, to enhance endogenous fibrinolysis, and tPA-mediated PDGFRα signaling, to decrease BBB damage, was more effective at reducing infarct size than either treatment alone.

A previous study in a rat model of embolic stroke has shown that Nsp delivery into the brain significantly reduces infarct size when administered along with intravenous tPA treatment [39]. This study showed that thrombolytic tPA, administered 4h after stroke onset, led to an increase in BBB leakage, and that Nsp reduced this effect of thrombolytic tPA on the BBB. In line with these findings, Gelderblom and collaborators report increased stroke size in $Nsp^{-/-}$ mice compared to WT mice in a transient MCAO model; however, the involvement of Nsp in BBB regulation and ICH was not studied [40]. In our data, we also compared double knockout mice, lacking both tPA and Nsp, to WT and $Nsp^{-/-}$ mice and these data demonstrate that the increased stroke size and BBB leakage observed in $Nsp^{-/-}$ mice following MCAO is primarily mediated by tPA since the Nsp-deficient phenotype is lost in the absence of tPA. It is important to point out that while in our model of stroke, the Nsp phenotype was mediated by tPA action, some studies have suggested that exogenous delivery of Nsp can exert a protective effect independent of tPA [41, 42]. However, this difference could be due to exogenous Nsp treatment reaching high non-physiological levels

of Nsp in the injected area that could inhibit other proteases such as uPA which has been shown to interact less efficiently with Nsp [15, 43].

A recent human study has shown that higher serum Nsp concentrations are associated with better clinical outcome in stroke patients [44]. In another study, patients treated with thrombolytic tPA who had high serum levels of neuroserpin before tPA administration were shown to have more favorable outcomes and a reduced probability of a subsequent parenchymal hematoma than patients with lower serum Nsp [45]. This apparently paradoxical result, that higher levels of a tPA inhibitor in blood are correlated with a better outcome following intravenous treatment with tPA, might be explained by the compartmentalized actions of tPA described here. Our data suggest that in healthy mice Nsp is largely restricted to the CNS. If this is also true in humans, then detecting significant levels of Nsp in serum may be a biomarker of high CNS expression of Nsp, which may inhibit the effects of thrombolytic tPA on the BBB. This would be similar to the results described above in the rat model of embolic stroke, where compared to rats treated with tPA alone, the injection of recombinant Nsp into the brain protected against pharmacologic tPA induced increases in BBB leakage, brain edema, and ischemic lesion volume [39]. It is also unlikely that the plasma levels of Nsp in these patients could have significantly impacted the thrombolytic activity of tPA in the blood since the highest level of Nsp reported by Rodríguez-González et al was 262ng/mL [45], while the tPA levels expected during thrombolytic therapy would be ~ 40-fold higher at ~10μg/mL (tPA dosed at 0.9mg/kg). Thus, given the single interaction mousetrap-like mechanism of serpin inhibitors [15, 24, 25], the Nsp in blood would have been rapidly consumed by tPA while reducing the tPA activity only slightly. However, the concentration of administered tPA that crossed into the perivascular space of the CNS would be much lower, whereas the CNS concentration of Nsp would be expected to be significantly higher than in the blood.

The role of PAI-1 in stroke has been extensively studied in different models of ischemic stroke, including a permanent MCA ligation model [46], a photothrombotic model [47], and a transient MCAO model [48], with results showing alternatively that PAI-1 deficiency increases infarct size, or decreases infarct size [48], and that PAI-1 overexpression either increases or decreases infarction depending on the model used [46–48]. In addition, the use of drugs and monoclonal antibodies targeting PAI-1 have been shown to have protective effects in mouse and rat models of ischemic stroke [49, 50]. In these studies, both transient and thrombotic models suggest that PAI-1 expression increases stroke damage. It is only in the permanent occlusion model were PAI-1 deficiency increased stroke damage and PAI-1 overexpression reduced stroke severity [47]. These data are similar to results in an *in vitro* model of the BBB where added PAI-1 enhanced barrier integrity [51]. The seemingly contradictory observations that PAI-1 can lead to infarct size reduction in the permanent MCA ligation model or enhance barrier integrity *in vitro* could be attributed to PAI-1-mediated effects on fibrinolysis not being a relevant factor in these models. Additionally, the protective phenotype of PAI-1 overexpression in the permanent MCA ligation model could be attributed to other PAI-1 functions independent of fibrinolysis or by PAI-1 extravasation to the CNS leading to inhibition of endogenous tPA's neurotoxic effects in the brain [47]. Our data using a photothrombotic MCAO model strongly suggest that endogenous PAI-1's primary effect is on the regulation of fibrinolysis. Specifically,

we showed that blocking fibrinolysis with the potent plasmin inhibitor aprotinin in PAI-1 deficient mice reverted the protective phenotype in PAI-$1^{-/-}$ mice and increased the infarct size similar to that seen in WT mice. This indicates that in PAI-$1^{-/-}$ mice enhanced endogenous fibrinolysis is mediating the reduction in infarct size after MCAO. However, it is unclear which plasminogen activator, tPA or uPA is driving fibrinolysis in the PAI-$1^{-/-}$ mice. *In vivo* experiments suggest that there is significant redundancy in the fibrinolytic response with both tPA and uPA [52], and in mouse models of stroke both tPA and uPA activity are upregulated at early time points suggesting that both plasminogen activators can contribute to fibrinolysis in the PAI-$1^{-/-}$ mice [48, 53]. Consistent with this, our data in figure 4a shows that tPA deficiency does not increase infarct size in the context of Nsp deficiency and in fact, is modestly protective. This suggests that with regard to fibrinolysis, uPA may compensate for the loss of tPA expression. Overall, our data support and expand previous studies suggesting that PAI-1 may be a potential therapeutic target to safely enhance endogenous fibrinolysis after stroke.

Our expression data for Nsp, tPA and PAI-1 suggests that in naïve WT mice there is a compartmentalization of the plasminogen activator inhibitors, Nsp in the CNS and PAI-1 in the blood. We demonstrated that PAI-1 was found primarily in the blood with low levels in the brain compared to Nsp. PAI-1 was not detected in cortical brain regions of naïve WT mice. In contrast, Nsp was highly expressed throughout the brain and was also associated with the parenchymal side of blood vessels and in proximity to tPA expressing perivascular cells. This is in good agreement with previous studies, describing the expression of Nsp in the mouse brain which demonstrated high levels of Nsp expression in neurons of the cortex, hippocampus and amygdala [11, 15, 54]. *In vitro* evidence suggests that Nsp is localized in large dense-core vesicles and is axonally secreted by neurons [55, 56]. Studies also show that overexpression of Nsp in neurons provides significant protection in stroke [57]. This suggests that Nsp released by neurons could be the main inhibitor regulating tPA's action in the brain. Although, recent evidence suggests that Nsp can also be expressed by different types of immune cells [58–60]. However, the extent of the involvement of Nsp expressed by these immune cells in stroke pathology has not been explored. The mRNA levels of Nsp were significantly higher than tPA in the brain, in good agreement with the reported differential gene expression analysis done in C57BL/6J mice [61]. However, we found that tPA protein levels in the brain were higher than Nsp, suggesting a higher turnover of Nsp in the brain. This could be explained by the single interaction mousetrap-like mechanism of Nsp and the relatively rapid turnover of the Nsp-tPA complex [24, 62]. Although the evolutionary basis of the compartmentalization and differential functions of PAI-1 and Nsp remain unknown, PAI-1 in the blood is known to be a potent inhibitor of both tPA and uPA [63, 64], making it an efficient inhibitor of fibrinolysis whereas Nsp inhibitory activity is significantly more selective for tPA compared to uPA [15]. This suggests that Nsp would not be as effective at regulating fibrinolysis driven by both tPA and uPA. Interestingly, recent reports have suggested that in the CNS uPA has protective activities following ischemic stroke [65, 66]. We hypothesize that unlike the regulation of fibrinolysis where tPA and uPA both act on the same substrate, plasminogen, in the CNS uPA and tPA may act on different substrates generating differential activities. In the case of tPA we suggest that an important substrate is PDGF-CC [10, 12, 67, 68]. For uPA it is not known what the substrate(s) might

be but we suggest that the compartmentalization of PAI-1 and Nsp in the blood and CNS, respectively may reflect the need to control the activity of different substrates acting on different pathways. Thus, PAI-1 can regulate fibrinolysis through its action on both uPA and tPA whereas Nsp can specifically target tPA without affecting uPA activity.

Finally, in this study, we have examined if understanding this compartmentalization would allow us to identify combined treatments that target both fibrinolysis and BBB dysfunction to improve stroke outcomes. To enhance endogenous fibrinolysis, we used our recently described small molecule PAI-1 inhibitor, MDI-2268 [20]. This compound has potent and selective inhibitory activity against PAI-1 and has been shown in mice to increase free tPA in plasma [69]. In addition, MDI-2268 has been reported to have robust *in vivo* antithrombotic activity without increasing bleeding risk [20, 70]. In the present study, we found that MDI-2268 treatment in WT mice was protective after MCAO with no increase in spontaneous ICH. Additionally, we combined this treatment with imatinib which we and others have previously shown to inhibit tPA-induced PDGFRα signaling and BBB dysfunction [10, 71, 72]. The combination treatment with MDI-2268 and imatinib targeting two non-overlapping pathways led to an additive benefit following MCAO, suggesting that increasing endogenous fibrinolysis while protecting the BBB from tPA-mediated damage in stroke has significant translational potential for the treatment of ischemic stroke. Finally, we showed that this combined treatment was also safe and effective when administered together with thrombolytic tPA.

Conclusions

In conclusion, our data show the beneficial and harmful effects of regulating two plasminogen activators inhibitors, PAI-1 and Nsp in the context of ischemic stroke. We took advantage of the differential function of tPA in the brain and blood and developed a combination therapy that offers additive protection in a photothrombotic MCAO mouse model of stroke. This was accomplished by increasing endogenous fibrinolysis and blocking tPA-mediated BBB disruption using a novel PAI-1 inhibitor and a PDGFRα inhibitor, respectively.

Supplementary Material

Refer to Web version on PubMed Central for supplementary material.

Acknowledgments

The Authors wish to thank Naga Sandhya Guntaka for work on the synthesis of MDI-2268.

Funding

The work was supported by the National Institutes of Health (HL055374 to DAL), and by the Eastern Michigan University Office of Research Development.

Abbreviations

tPA	Tissue plasminogen activator

CNS	Central nervous system
BBB	Blood brain barrier
PAI-1	Plasminogen activator inhibitor 1
Nsp	Neuroserpin
PDGF-CC	Platelet-derived growth factor CC
PDGFRα	PDGF receptor α
MCAO	Middle cerebral artery occlusion
ICH	Intra cerebral hemorrhage
MCA	Middle cerebral artery
CBF	Cerebral Blood flow
TTC	2,3,5-triphenyltetrazolium chloride
TMB	3,3’,5,5’-tetramethylbenzidine
uPA	Urokinase plasminogen activator

References

1. Johnson CO, Nguyen M, Roth GA, Nichols E, Alam T, Abate D, et al. Global, regional, and national burden of stroke, 1990–2016: a systematic analysis for the Global Burden of Disease Study 2016. The Lancet Neurology. 2019;18(5):439–58. [PubMed: 30871944]
2. Virani SS, Alonso A, Aparicio HJ, Benjamin EJ, Bittencourt MS, Callaway CW, et al. Heart Disease and Stroke Statistics-2021 Update: A Report From the American Heart Association. Circulation. 2021;143(8):e254–e743. [PubMed: 33501848]
3. Andersen Klaus K, Olsen Tom S, Dehlendorff C, Kammersgaard Lars P. Hemorrhagic and Ischemic Strokes Compared. Stroke. 2009;40(6):2068–72. [PubMed: 19359645]
4. Yu WM, Abdul-Rahim AH, Cameron AC, Korv J, Sevcik P, Toni D, et al. The Incidence and Associated Factors of Early Neurological Deterioration After Thrombolysis: Results From SITS Registry. Stroke. 2020;51(9):2705–14. [PubMed: 32811373]
5. Yaghi S, Willey Joshua Z, Cucchiara B, Goldstein Joshua N, Gonzales Nicole R, Khatri P, et al. Treatment and Outcome of Hemorrhagic Transformation After Intravenous Alteplase in Acute Ischemic Stroke: A Scientific Statement for Healthcare Professionals From the American Heart Association/American Stroke Association. Stroke. 2017;48(12):e343–e61. [PubMed: 29097489]
6. Zhang J, Yang Y, Sun H, Xing Y. Hemorrhagic transformation after cerebral infarction: current concepts and challenges. Ann Transl Med. 2014;2(8):81. [PubMed: 25333056]
7. Sweeney MD, Zhao Z, Montagne A, Nelson AR, Zlokovic BV. Blood-Brain Barrier: From Physiology to Disease and Back. Physiological Reviews. 2019;99(1):21–78. [PubMed: 30280653]
8. Jiang X, Andjelkovic AV, Zhu L, Yang T, Bennett MVL, Chen J, et al. Blood-brain barrier dysfunction and recovery after ischemic stroke. Progress in Neurobiology. 2018;163–164:144–71.
9. Yepes M, Sandkvist M, Moore EG, Bugge TH, Strickland DK, Lawrence DA. Tissue-type plasminogen activator induces opening of the blood-brain barrier via the LDL receptor-related protein. J Clin Invest. 2003;112(10):1533–40. [PubMed: 14617754]
10. Su EJ, Fredriksson L, Geyer M, Folestad E, Cale J, Andrae J, et al. Activation of PDGF-CC by tissue plasminogen activator impairs blood-brain barrier integrity during ischemic stroke. Nature Medicine. 2008;14(7):731–7.

11. Fredriksson L, Stevenson TK, Su EJ, Ragsdale M, Moore S, Craciun S, et al. Identification of a neurovascular signaling pathway regulating seizures in mice. Annals of Clinical and Translational Neurology. 2015;2(7):722–38. [PubMed: 26273685]
12. Su EJ, Cao C, Fredriksson L, Nilsson I, Stefanitsch C, Stevenson TK, et al. Microglial-mediated PDGF-CC activation increases cerebrovascular permeability during ischemic stroke. Acta Neuropathol. 2017;134(4):585–604. [PubMed: 28725968]
13. Wahlgren N, Thorén M, Höjeberg B, Käll TB, Laska AC, Sjöstrand C, et al. Randomized assessment of imatinib in patients with acute ischaemic stroke treated with intravenous thrombolysis. J Intern Med. 2017;281(3):273–83. [PubMed: 27862464]
14. Tjärnlund-Wolf A, Brogren H, Lo EH, Wang X. Plasminogen Activator Inhibitor-1 and Thrombotic Cerebrovascular Diseases. Stroke. 2012;43(10):2833–9. [PubMed: 22879095]
15. Hastings GA, Coleman TA, Haudenschild CC, Stefansson S, Smith EP, Barthlow R, et al. Neuroserpin, a brain-associated inhibitor of tissue plasminogen activator is localized primarily in neurons. Implications for the regulation of motor learning and neuronal survival. J Biol Chem. 1997;272(52):33062–7. [PubMed: 9407089]
16. Lee TW, Tsang VW, Loef EJ, Birch NP. Physiological and pathological functions of neuroserpin: Regulation of cellular responses through multiple mechanisms. Semin Cell Dev Biol. 2017;62:152–9. [PubMed: 27639894]
17. Madani R, Kozlov S, Akhmedov A, Cinelli P, Kinter J, Lipp HP, et al. Impaired explorative behavior and neophobia in genetically modified mice lacking or overexpressing the extracellular serine protease inhibitor neuroserpin. Mol Cell Neurosci. 2003;23(3):473–94. [PubMed: 12837630]
18. Carmeliet P, Kieckens L, Schoonjans L, Ream B, van Nuffelen A, Prendergast G, et al. Plasminogen activator inhibitor-1 gene-deficient mice. I. Generation by homologous recombination and characterization. J Clin Invest. 1993;92(6):2746–55. [PubMed: 8254028]
19. Szabo R, Samson AL, Lawrence DA, Medcalf RL, Bugge TH. Passenger mutations and aberrant gene expression in congenic tissue plasminogen activator-deficient mouse strains. J Thromb Haemost. 2016;14(8):1618–28. [PubMed: 27079292]
20. Reinke AA, Li SH, Warnock M, Shaydakov ME, Guntaka NS, Su EJ, et al. Dual-reporter high-throughput screen for small-molecule in vivo inhibitors of plasminogen activator inhibitor type-1 yields a clinical lead candidate. J Biol Chem. 2019;294(5):1464–77. [PubMed: 30510136]
21. Stevenson TK, Lawrence DA. Characterization of Tissue Plasminogen Activator Expression and Trafficking in the Adult Murine Brain. eneuro. 2018;5(4):ENEURO.0119–18.2018.
22. Courey AJ, Horowitz JC, Kim KK, Koh TJ, Novak ML, Subbotina N, et al. The vitronectin-binding function of PAI-1 exacerbates lung fibrosis in mice. Blood. 2011;118(8):2313–21. [PubMed: 21734232]
23. Zuo Y, Warnock M, Harbaugh A, Yalavarthi S, Gockman K, Zuo M, et al. Plasma tissue plasminogen activator and plasminogen activator inhibitor-1 in hospitalized COVID-19 patients. Sci Rep. 2021;11(1):1580-. [PubMed: 33452298]
24. Barker-Carlson K, Lawrence DA, Schwartz BS. Acyl-enzyme complexes between tissue-type plasminogen activator and neuroserpin are short-lived in vitro. J Biol Chem. 2002;277(49):46852–7. [PubMed: 12228252]
25. Sanrattana W, Maas C, de Maat S. SERPINs—From Trap to Treatment. Frontiers in Medicine. 2019;6:25. [PubMed: 30809526]
26. Izuhara Y, Yamaoka N, Kodama H, Dan T, Takizawa S, Hirayama N, et al. A Novel Inhibitor of Plasminogen Activator Inhibitor-1 Provides Antithrombotic Benefits Devoid of Bleeding Effect in Nonhuman Primates. J Cereb Blood Flow Metab. 2010;30(5):904–12. [PubMed: 20087372]
27. Hennan JK, Morgan GA, Swillo RE, Antrilli TM, Mugford C, Vlasuk GP, et al. Effect of tiplaxtinin (PAI-039), an orally bioavailable PAI-1 antagonist, in a rat model of thrombosis. J Thromb Haemost. 2008;6(9):1558–64. [PubMed: 18624980]
28. Kwiatkowski TG, Libman RB, Frankel M, Tilley BC, Morgenstern LB, Lu M, et al. Effects of tissue plasminogen activator for acute ischemic stroke at one year. National Institute of Neurological Disorders and Stroke Recombinant Tissue Plasminogen Activator Stroke Study Group. N Engl J Med. 1999;340(23):1781–7. [PubMed: 10362821]

29. Gonzales NR, Grotta JC. Alteplase for acute ischemic stroke. Expert Review of Cardiovascular Therapy. 2006;4(3):301–18. [PubMed: 16716092]
30. Zhang ZG, Chopp M, Goussev A, Lu D, Morris D, Tsang W, et al. Cerebral microvascular obstruction by fibrin is associated with upregulation of PAI-1 acutely after onset of focal embolic ischemia in rats. J Neurosci. 1999;19(24):10898–907. [PubMed: 10594071]
31. Reed GL, Houng AK, Wang D. Microvascular thrombosis, fibrinolysis, ischemic injury, and death after cerebral thromboembolism are affected by levels of circulating alpha2-antiplasmin. Arterioscler Thromb Vasc Biol. 2014;34(12):2586–93. [PubMed: 25256235]
32. Su EJ, Lawrence DA. alpha2 Antiplasmin and microvascular thrombosis in ischemic stroke. Arterioscler Thromb Vasc Biol. 2014;34(12):2522–3. [PubMed: 25411105]
33. Mazya M, Egido JA, Ford GA, Lees KR, Mikulik R, Toni D, et al. Predicting the risk of symptomatic intracerebral hemorrhage in ischemic stroke treated with intravenous alteplase: safe Implementation of Treatments in Stroke (SITS) symptomatic intracerebral hemorrhage risk score. Stroke. 2012;43(6):1524–31. [PubMed: 22442178]
34. Zhang Y, Wang Y, Zuo Z, Wang Z, Roy J, Hou Q, et al. Effects of tissue plasminogen activator timing on blood-brain barrier permeability and hemorrhagic transformation in rats with transient ischemic stroke. J Neurol Sci. 2014;347(1–2):148–54. [PubMed: 25292413]
35. Boese AC, Eckert A, Hamblin MH, Lee JP. Human neural stem cells improve early stage stroke outcome in delayed tissue plasminogen activator-treated aged stroke brains. Exp Neurol. 2020;329:113275. [PubMed: 32147438]
36. Prabhakaran S, Ruff I, Bernstein RA. Acute stroke intervention: a systematic review. JAMA. 2015;313(14):1451–62. [PubMed: 25871671]
37. Hacke W, Lyden P, Emberson J, Baigent C, Blackwell L, Albers G, et al. Effects of alteplase for acute stroke according to criteria defining the European Union and United States marketing authorizations: Individual-patient-data meta-analysis of randomized trials. Int J Stroke. 2018;13(2):175–89. [PubMed: 29171359]
38. Kleindorfer D, de los Rios La Rosa F, Khatri P, Kissela B, Mackey J, Adeoye O. Temporal trends in acute stroke management. Stroke. 2013;44(6 Suppl 1):S129–31. [PubMed: 23709709]
39. Zhang Z, Zhang L, Yepes M, Jiang Q, Li Q, Arniego P, et al. Adjuvant Treatment With Neuroserpin Increases the Therapeutic Window for Tissue-Type Plasminogen Activator Administration in a Rat Model of Embolic Stroke. Circulation. 2002;106(6):740–5. [PubMed: 12163437]
40. Gelderblom M, Neumann M, Ludewig P, Bernreuther C, Krasemann S, Arunachalam P, et al. Deficiency in Serine Protease Inhibitor Neuroserpin Exacerbates Ischemic Brain Injury by Increased Postischemic Inflammation. PLOS ONE. 2013;8(5):e63118. [PubMed: 23658802]
41. Gu RP, Fu LL, Jiang CH, Xu YF, Wang X, Yu J. Retina Is Protected by Neuroserpin from Ischemic/Reperfusion-Induced Injury Independent of Tissue-Type Plasminogen Activator. PLOS ONE. 2015;10(7):e0130440. [PubMed: 26176694]
42. Wu J, Echeverry R, Guzman J, Yepes M. Neuroserpin Protects Neurons from Ischemia-Induced Plasmin-Mediated Cell Death Independently of Tissue-Type Plasminogen Activator Inhibition. Am J Pathol. 2010;177(5):2576–84. [PubMed: 20864675]
43. Osterwalder T, Cinelli P, Baici A, Pennella A, Krueger SR, Schrimpf SP, et al. The axonally secreted serine proteinase inhibitor, neuroserpin, inhibits plasminogen activators and plasmin but not thrombin. J Biol Chem. 1998;273(4):2312–21. [PubMed: 9442076]
44. Wu W, Asakawa T, Yang Q, Zhao J, Lu L, Luo Y, et al. Effects of neuroserpin on clinical outcomes and inflammatory markers in Chinese patients with acute ischemic stroke. Neurol Res. 2017;39(10):862–8. [PubMed: 28738762]
45. Rodriguez-Gonzalez R, Millan M, Sobrino T, Miranda E, Brea D, de la Ossa NP, et al. The natural tissue plasminogen activator inhibitor neuroserpin and acute ischaemic stroke outcome. Thromb Haemost. 2011;105(3):421–9. [PubMed: 21174006]
46. Nagai N, De Mol M, Lijnen HR, Carmeliet P, Collen D. Role of plasminogen system components in focal cerebral ischemic infarction: a gene targeting and gene transfer study in mice. Circulation. 1999;99(18):2440–4. [PubMed: 10318667]

47. Nagai N, Suzuki Y, Van Hoef B, Lijnen HR, Collen D. Effects of plasminogen activator inhibitor-1 on ischemic brain injury in permanent and thrombotic middle cerebral artery occlusion models in mice. J Thromb Haemost. 2005;3(7):1379–84. [PubMed: 15978095]
48. Griemert E-V, Recarte Pelz K, Engelhard K, Schäfer MK, Thal SC. PAI-1 but Not PAI-2 Gene Deficiency Attenuates Ischemic Brain Injury After Experimental Stroke. Translational Stroke Research. 2019;10(4):372–80. [PubMed: 29978354]
49. Chan S-L, Bishop N, Li Z, Cipolla MJ. Inhibition of PAI (Plasminogen Activator Inhibitor)-1 Improves Brain Collateral Perfusion and Injury After Acute Ischemic Stroke in Aged Hypertensive Rats. Stroke. 2018;49(8):1969–76. [PubMed: 29991657]
50. Denorme F, Wyseure T, Peeters M, Vandeputte N, Gils A, Deckmyn H, et al. Inhibition of Thrombin-Activatable Fibrinolysis Inhibitor and Plasminogen Activator Inhibitor-1 Reduces Ischemic Brain Damage in Mice. Stroke. 2016;47(9):2419–22. [PubMed: 27470988]
51. Dohgu S, Takata F, Matsumoto J, Oda M, Harada E, Watanabe T, et al. Autocrine and paracrine up-regulation of blood-brain barrier function by plasminogen activator inhibitor-1. Microvasc Res. 2011;81(1):103–7. [PubMed: 21036181]
52. Carmeliet P, Schoonjans L, Kieckens L, Ream B, Degen J, Bronson R, et al. Physiological consequences of loss of plasminogen activator gene function in mice. Nature. 1994;368(6470):419–24. [PubMed: 8133887]
53. Yepes M, Sandkvist M, Wong MKK, Coleman TA, Smith E, Cohan SL, et al. Neuroserpin reduces cerebral infarct volume and protects neurons from ischemia-induced apoptosis. Blood. 2000;96(2):569–76. [PubMed: 10887120]
54. Krueger SR, Ghisu GP, Cinelli P, Gschwend TP, Osterwalder T, Wolfer DP, et al. Expression of neuroserpin, an inhibitor of tissue plasminogen activator, in the developing and adult nervous system of the mouse. J Neurosci. 1997;17(23):8984–96. [PubMed: 9364046]
55. Osterwalder T, Contartese J, Stoeckli ET, Kuhn TB, Sonderegger P. Neuroserpin, an axonally secreted serine protease inhibitor. EMBO J. 1996;15(12):2944–53. [PubMed: 8670795]
56. Ishigami S, Sandkvist M, Tsui F, Moore E, Coleman TA, Lawrence DA. Identification of a novel targeting sequence for regulated secretion in the serine protease inhibitor neuroserpin. Biochem J. 2007;402(1):25–34. [PubMed: 17040209]
57. Cinelli P, Madani R, Tsuzuki N, Vallet P, Arras M, Zhao CN, et al. Neuroserpin, a neuroprotective factor in focal ischemic stroke. Mol Cell Neurosci. 2001;18(5):443–57. [PubMed: 11922137]
58. Kennedy SA, van Diepen AC, van den Hurk CM, Coates LC, Lee TW, Ostrovsky LL, et al. Expression of the serine protease inhibitor neuroserpin in cells of the human myeloid lineage. Thromb Haemost. 2007;97(3):394–9. [PubMed: 17334506]
59. Lorenz N, Loef EJ, Verdon DJ, Chen CJ, Mansell CJ, Angel CE, et al. Human T cell activation induces synaptic translocation and alters expression of the serine protease inhibitor neuroserpin and its target protease. J Leukoc Biol. 2015;97(4):699–710. [PubMed: 25670787]
60. Loef EJ, Brooks AES, Lorenz N, Birch NP, Dunbar PR. Neuroserpin regulates human T cell-T cell interactions and proliferation through inhibition of tissue plasminogen activator. J Leukoc Biol. 2020;107(1):145–58. [PubMed: 31667914]
61. Papatheodorou I, Moreno P, Manning J, Fuentes AM-P, George N, Fexova S, et al. Expression Atlas update: from tissues to single cells. Nucleic Acids Research. 2020;48(D1):D77–D83. [PubMed: 31665515]
62. Carlson KS, Nguyen L, Schwartz K, Lawrence DA, Schwartz BS. Neuroserpin Differentiates Between Forms of Tissue Type Plasminogen Activator via pH Dependent Deacylation. Front Cell Neurosci. 2016;10:154. [PubMed: 27378851]
63. van Mourik JA, Lawrence DA, Loskutoff DJ. Purification of an inhibitor of plasminogen activator (antiactivator) synthesized by endothelial cells. J Biol Chem. 1984;259(23):14914–21. [PubMed: 6438106]
64. Lawrence D, Strandberg L, Grundstrom T, Ny T. Purification of active human plasminogen activator inhibitor 1 from Escherichia coli. Comparison with natural and recombinant forms purified from eucaryotic cells. Eur J Biochem. 1989;186(3):523–33. [PubMed: 2514093]

65. Diaz A, Merino P, Manrique LG, Cheng L, Yepes M. Urokinase-type plasminogen activator (uPA) protects the tripartite synapse in the ischemic brain via ezrin-mediated formation of peripheral astrocytic processes. J Cereb Blood Flow Metab. 2019;39(11):2157–71. [PubMed: 29890880]

66. Wu F, Catano M, Echeverry R, Torre E, Haile WB, An J, et al. Urokinase-type plasminogen activator promotes dendritic spine recovery and improves neurological outcome following ischemic stroke. J Neurosci. 2014;34(43):14219–32. [PubMed: 25339736]

67. Fredriksson L, Li H, Fieber C, Li X, Eriksson U. Tissue plasminogen activator is a potent activator of PDGF-CC. EMBO J. 2004;23(19):3793–802. [PubMed: 15372073]

68. Fredriksson L, Lawrence DA, Medcalf RL. tPA Modulation of the Blood-Brain Barrier: A Unifying Explanation for the Pleiotropic Effects of tPA in the CNS. Semin Thromb Hemost. 2017;43(2):154–68. [PubMed: 27677179]

69. Kaiko GE, Chen F, Lai CW, Chiang IL, Perrigoue J, Stojmirović A, et al. PAI-1 augments mucosal damage in colitis. Sci Transl Med. 2019;11(482).

70. Shaydakov M, Rainey J, Lawrence D, Diaz J. First Use of a Novel Inhibitor of Plasminogen Activator Inhibitor 1 (MDI-2268) in Animal Model of Deep Venous Thrombosis and Attempts of Combined Antithrombotic Therapy. Journal of Vascular Surgery: Venous and Lymphatic Disorders. 2020;8(2):309–10.

71. Ma Q, Huang B, Khatibi N, Rolland II W, Suzuki H, Zhang JH, et al. PDGFR-α inhibition preserves blood-brain barrier after intracerebral hemorrhage. Annals of Neurology. 2011;70(6):920–31. [PubMed: 22190365]

72. Su E, Fredriksson L, Kanzawa M, Moore S, Folestad E, Stevenson T, et al. Imatinib treatment reduces brain injury in a murine model of traumatic brain injury. Front Cell Neurosci. 2015;9(385).

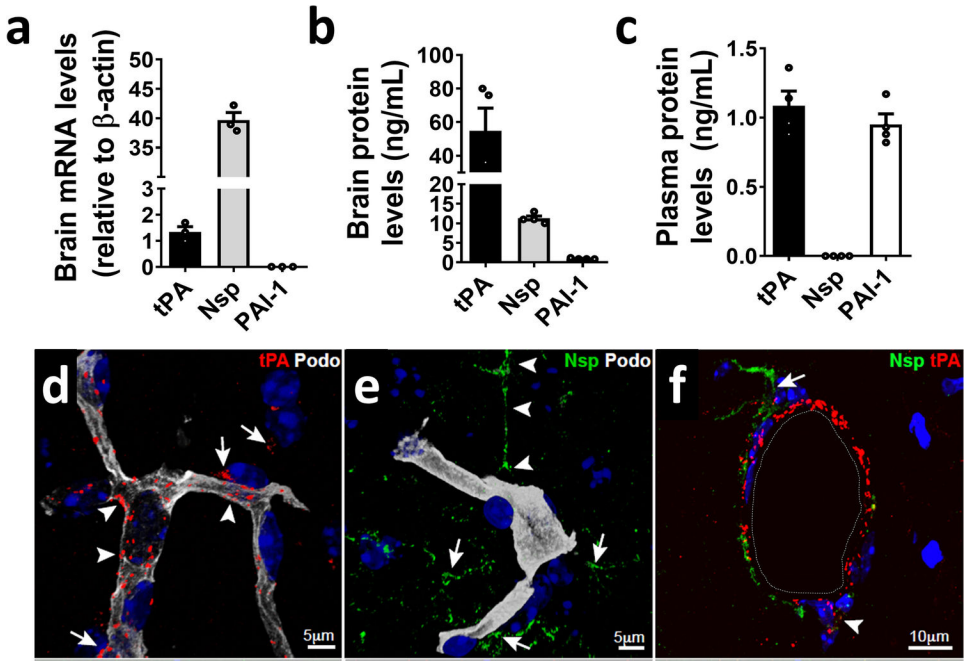

Figure 1. Expression of tPA, Nsp and PAI-1 in brain and blood.

(a) mRNA levels of tPA, Nsp and PAI-1 in brain tissue were quantified by qPCR in naïve WT mice, showing a prevalence of Nsp expression in the brain whereas PAI-1 levels were undetected (n=3). (b-c) Protein levels of tPA, Nsp and PAI-1 in plasma and brain were measured by ELISA (Nsp) or Luminex assay (tPA and PAI-1; n=4). (d-f) Confocal images of cortical brain regions in the mouse brain showing tPA (red), podocalyxin (white) and Nsp (green). (d) tPA localization in the vessel wall (stained with podocalyxin; arrowheads) and in the brain parenchyma (long arrows). (e) Nsp immunoreactivity in cells associated with cerebral vessels (arrowheads) and in the brain parenchyma (long arrows). (f) Double staining of tPA and Nsp showing both proteins are expressed around a cerebral vessel with the vessel lumen outlined with the dashed white line. Data is shown as mean values ± SEM.

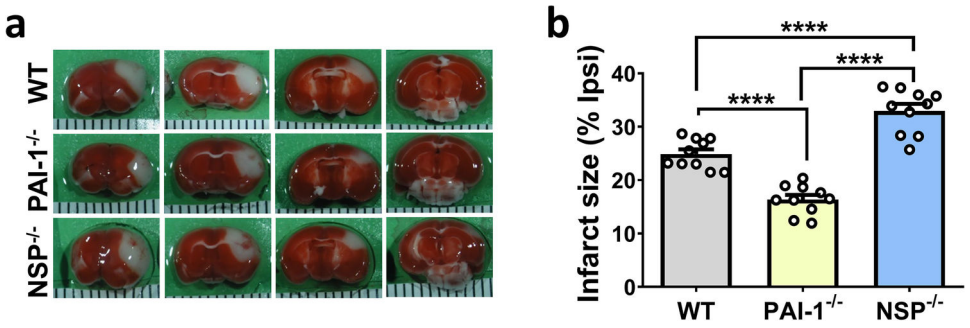

Figure 2. Nsp and PAI-1 deficiency have opposite effects on infarct size after MCAO.

(a) Representative images of TTC staining of serial coronal sections of the mouse brain 72h after photothrombotic MCAO in WT, PAI-1$^{-/-}$ and Nsp$^{-/-}$ mice. (b) Quantification of infarct size in WT, PAI-1$^{-/-}$ and Nsp$^{-/-}$ mice 72h after MCAO showing opposite effects on infarct size in Nsp and PAI-1 deficient mice compared to WT mice (n=10). Data is shown as mean values ± SEM, ****p<0.0001. 1-way ANOVA followed by Tukey post hoc test.

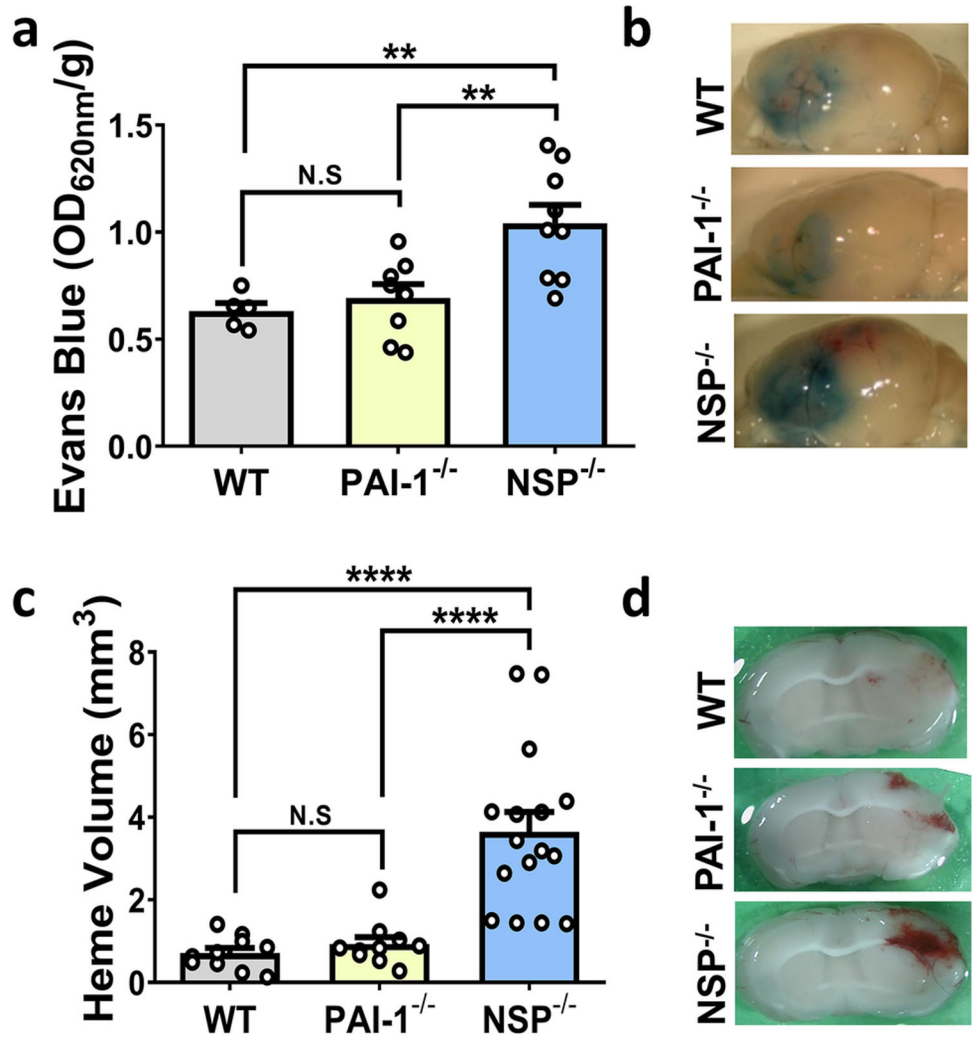

Figure 3. Nsp deficiency but not PAI-1 deficiency increases BBB opening after MCAO.

(a) BBB permeability was determined by quantitative Evans Blue assay 24h after photothrombotic MCAO and 1h after Evans blue tail vein injection (n=5–9). (b) Representative images of Evans blue in the infarct hemisphere 1h after Evans blue tail vein injection in WT, PAI-1$^{-/-}$ and Nsp$^{-/-}$ mice. (c) Intracerebral hemorrhage (ICH) volume was assessed at 72h after MCAO in serial coronal brain sections (n=10–16). (d) Representative images of coronal brain sections 72h after MCAO of WT, PAI-1$^{-/-}$ and Nsp$^{-/-}$ mice showing ICH. Data is shown as mean values ± SEM, N.S=not significant, **p<0.01; ****p<0.0001. 1-way ANOVA followed by Tukey post hoc test.

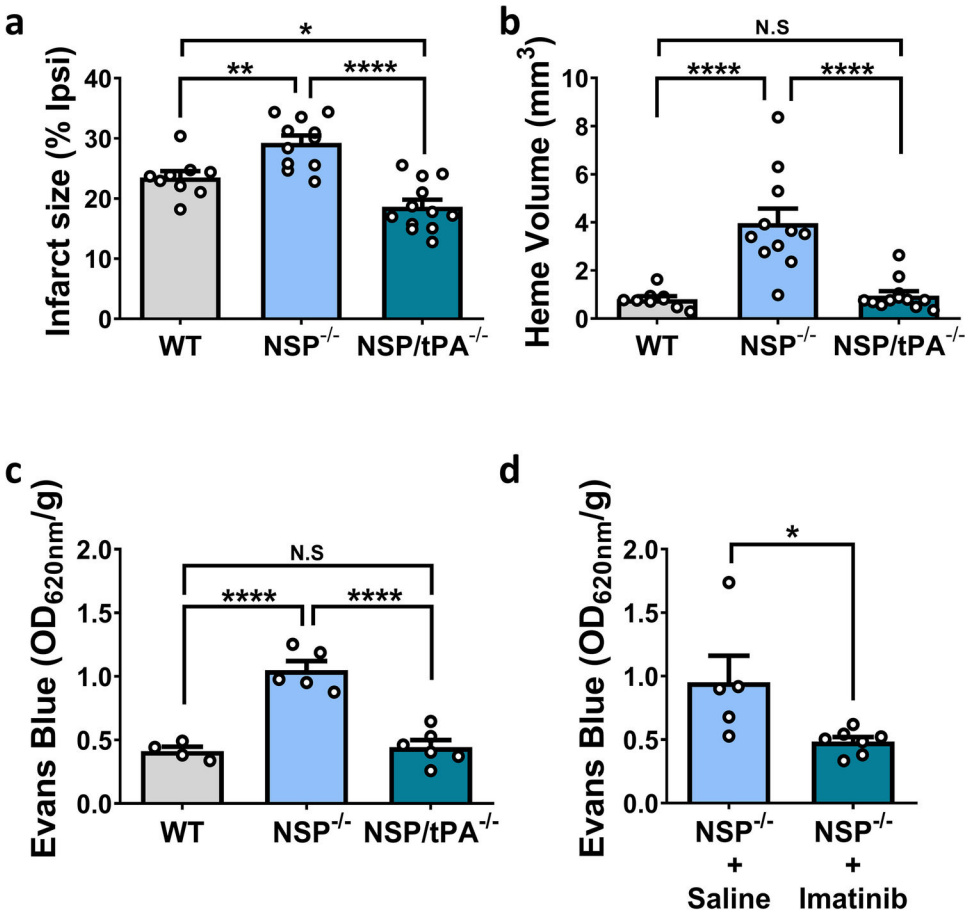

Figure 4. tPA mediates the increase in infarct size and BBB opening in Nsp deficient mice.

Quantification of infarct size (a) and ICH (b) in WT, Nsp$^{-/-}$ and Nsp/tPA$^{-/-}$ mice 72h after MCAO showing a reduction in both infarct size and spontaneous hemorrhage in Nsp/tPA$^{-/-}$ mice compared to Nsp$^{-/-}$ mice (n=9–12). (c) BBB disruption determined by quantitative Evans Blue analysis 24h after MCAO and 1h after Evans blue tail vein injection in WT, Nsp$^{-/-}$ and Nsp/tPA$^{-/-}$ mice, showing protection of the BBB in Nsp/tPA$^{-/-}$ mice compared to Nsp$^{-/-}$ mice (n=4–6). (d) Evans Blue quantification 24h after MCAO and 1h after Evans blue tail vein injection in Nsp$^{-/-}$ mice treated with the PDGFRα inhibitor imatinib or vehicle (oral gavage twice daily; n=5–7). Data is shown as mean values ± SEM, N.S=not significant, *p<0.05; **p<0.01; ****p<0.0001. (a-c) 1-way ANOVA followed by Tukey post hoc test, (d) 2-tailed t-test.

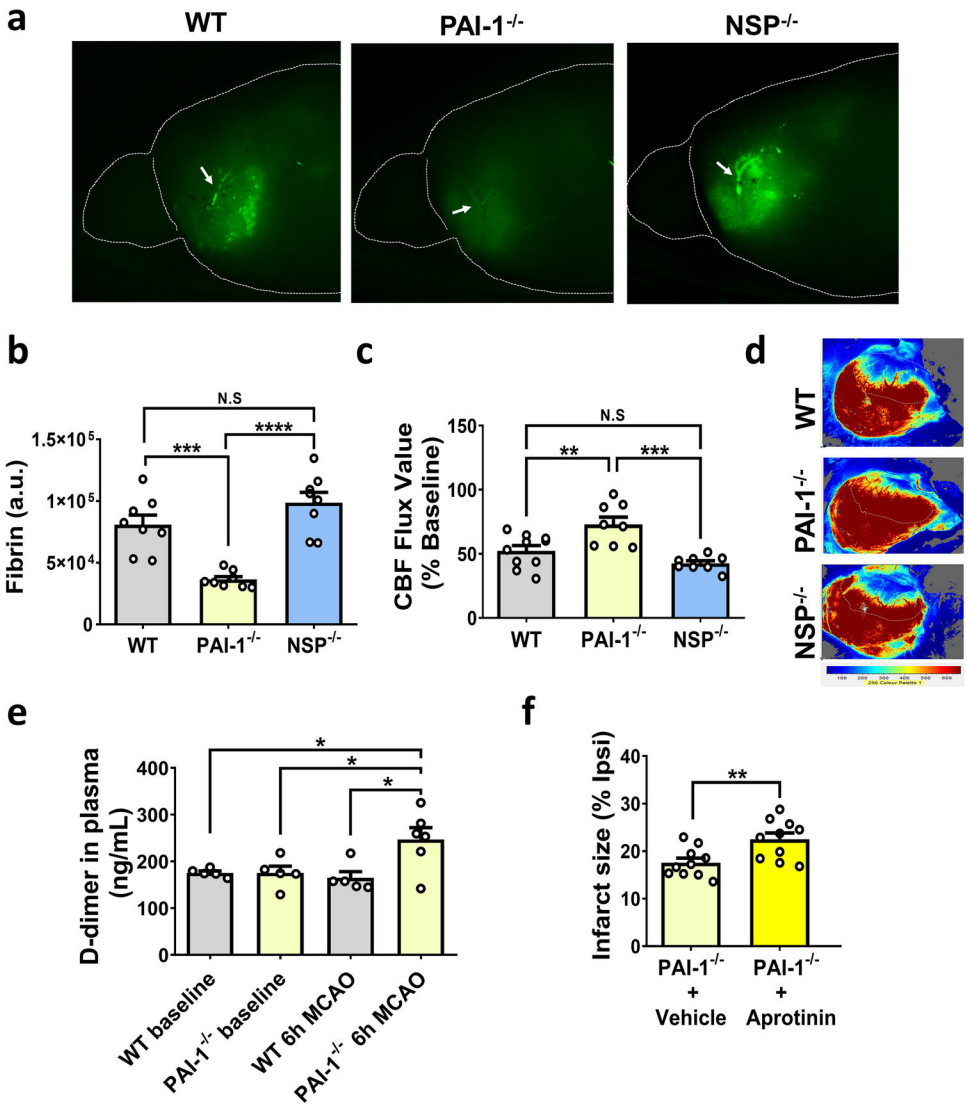

Figure 5. PAI-1 deficiency improves reperfusion after MCAO by increasing fibrinolysis.

(a-b) FITC-conjugated mouse fibrinogen (0.3mg/kg) was injected intravenously 10 minutes before MCAO in WT, Nsp$^{-/-}$ and PAI-1$^{-/-}$ mice. (a) Side view of perfused whole brain 3h after MCAO showing diffuse FITC-fibrin deposition in the ischemic hemisphere. The arrow indicates FITC-fibrin clots. (b) Quantification of side view FITC-fibrin deposition in the ischemic hemisphere 3h after MCAO in WT, PAI-1$^{-/-}$ and Nsp$^{-/-}$ mice (n=8). (c-d) Representative laser speckle images (d) and quantification (c) of CBF in WT, PAI-1$^{-/-}$ and Nsp$^{-/-}$ mice 24h after photothrombotic MCAO (n=8–10). Red and blue colors in d indicate normal and severely reduced CBF values, respectively. (e) Quantification of D-dimer in plasma of naïve WT and PAI-1$^{-/-}$ mice; and WT and PAI-1$^{-/-}$ mice 6h after MCAO (n=5–6). (f) Quantification of infarct size 72h after MCAO in PAI-1$^{-/-}$ mice treated with the plasmin inhibitor aprotinin or vehicle (I.P, 10 mg/Kg; twice daily) (n=10). Data is shown as mean values ± SEM, N.S=not significant, *p<0.05; **p<0.01; ***p<0.001; ****p<0.0001. (b, c, e) 1-way ANOVA followed by Tukey post hoc test, (f) 2-tailed t-test.

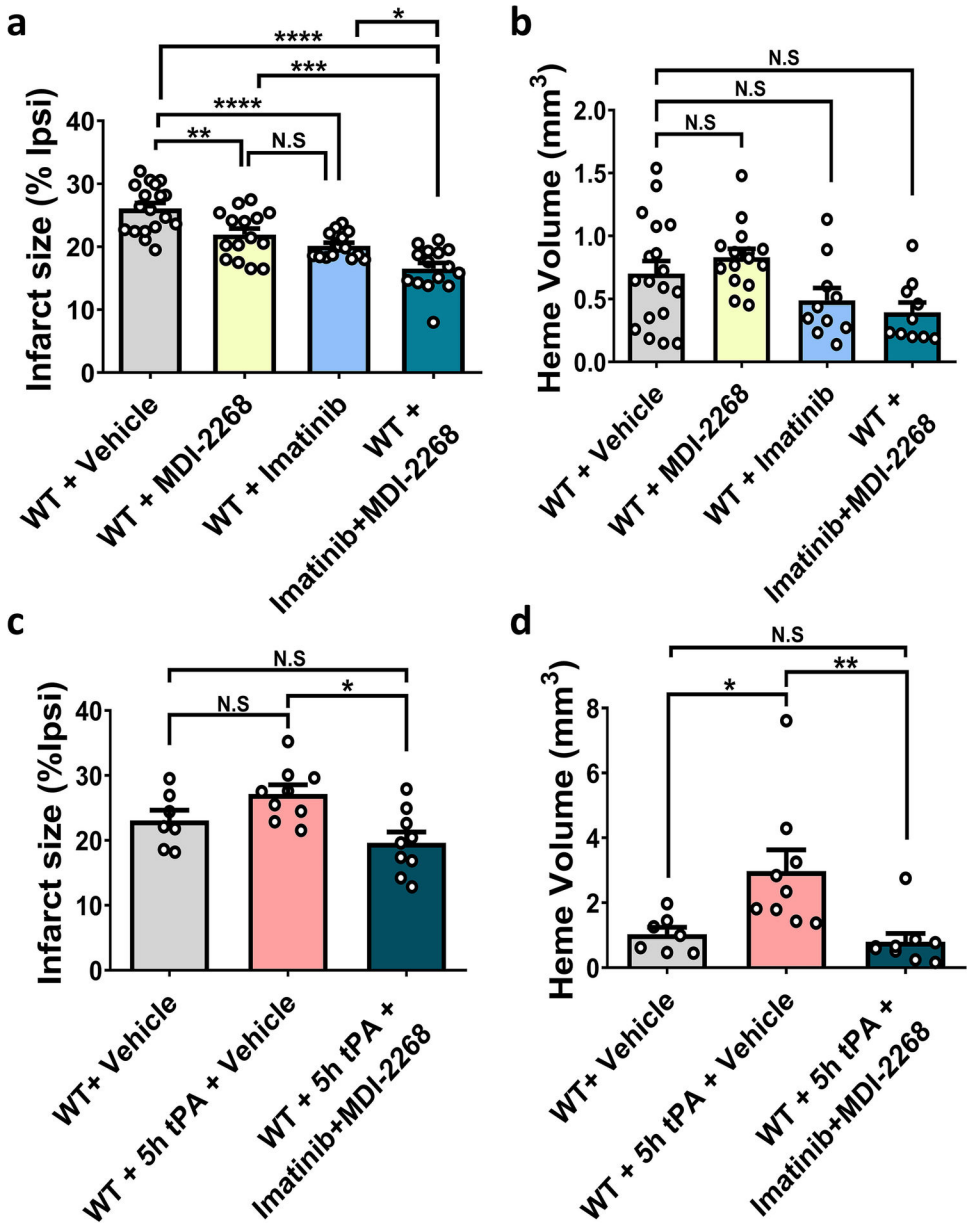

Figure 6. Combined pharmacological inhibition of PAI-1 and the tPA-Nsp pathway is safe and shows additive protection of the infarct zone after MCAO in WT mice.

(a-b) WT mice were subjected to MCAO and 30min later the PAI-1 inhibitor (MDI-2268; 3mg/kg, I.P.), or the PDGFRα inhibitor (imatinib; 300mg/kg, oral gavage), or a combined treatment of MDI-2268 and imatinib were administered twice daily for three days. (a) Quantification of infarct size was measured 72h by TTC staining. (b) ICH volumes were assessed at 72h after MCAO, (n=15–18). (c-d) WT mice were subjected to MCAO and 30min later a combined treatment of MDI-2268 and imatinib was administered and continued twice daily for three days (MDI-2268; 3mg/kg; imatinib; 300mg/kg). At 5h after MCAO, a single dose of human tPA (10 mg/kg, I.V.) or vehicle was administered. (c) Quantification of infarct sizes were determined at 72h by TTC staining. (d) ICH volumes were assessed at 72h after MCAO, (n=7–9). Data is shown as mean values ± SEM, N.S=not

significant, *p<0.05; **p<0.01; ***p<0.001; ****p<0.0001. 1-way ANOVA followed by Tukey post hoc test.